

# Coherent molecule formation in anharmonic potentials near confinement-induced resonances

S. Sala,<sup>1</sup> G. Zürn,<sup>2,3</sup> T. Lompe,<sup>2,3,4</sup> A. N. Wenz,<sup>2,3</sup> S. Murmann,<sup>2,3</sup> F. Serwane,<sup>2,3,4,5</sup> S. Jochim,<sup>2,3,4</sup> and A. Saenz<sup>1</sup>

<sup>1</sup>*AG Moderne Optik, Institut für Physik, Humboldt-Universität zu Berlin, Newtonstrasse 15, 12489 Berlin, Germany\**

<sup>2</sup>*Physikalisches Institut, Ruprecht-Karls-Universität Heidelberg, Germany*

<sup>3</sup>*Max-Planck-Institut für Kernphysik, Saupfercheckweg 1, 69117 Heidelberg, Germany*

<sup>4</sup>*ExtreMe Matter Institute EMMI, GSI Helmholtzzentrum für Schwerionenforschung, Darmstadt, Germany*

<sup>5</sup>*Now at the European Molecular Biology Laboratory, 69117 Heidelberg, Germany*

(Dated: April 22, 2022)

We perform a theoretical and experimental study of a system of two ultracold atoms with tunable interaction in an elongated trapping potential. We show that the coupling of center-of-mass and relative motion due to an anharmonicity of the trapping potential leads to a coherent coupling of a state of an unbound atom pair and a molecule with a center of mass excitation. By performing the experiment with exactly two particles we exclude three-body losses and can therefore directly observe coherent molecule formation. We find quantitative agreement between our theory of inelastic confinement-induced resonances and the experimental results. This shows that the effects of center-of-mass to relative motion coupling can have a significant impact on the physics of quasi-1D quantum systems.

A key question in condensed matter physics is how the dimensionality of a quantum system determines its physical properties. Especially in one dimension the increased role of quantum fluctuations leads to the appearance of interesting phenomena which cannot be observed in higher-dimensional systems. This poses the interesting question of how to experimentally realize such one-dimensional (1D) systems in a three-dimensional (3D) world. This can be achieved by confining particles in a strongly anisotropic potential whose lowest transversal excitation is much larger than all other relevant energy scales of the system. In this case a 3D system can be mapped onto a true 1D system obtaining an effective 1D coupling constant  $g_{1D}$  which depends on the 3D scattering length  $a$  [1]. In such anisotropic confinement, ultracold atoms have been used to study, e.g., the Tonks-Girardeau [2–4] and super-Tonks-Girardeau [5] gas as well as the fundamental question of what constitutes an integrable quantum system [6].

Such experiments [5, 7–10] often rely on the fact that it is possible to control the effective 1D coupling strength  $g_{1D}$  by tuning the scattering length  $a$  with a Feshbach resonance [11]. For a specific ratio of the scattering length and the transversal confinement length  $d_{\perp}$ ,  $g_{1D}$  diverges to  $\pm\infty$  at a confinement-induced resonance (CIR) [1]. To distinguish these resonances in the elastic scattering channel from the molecule-formation resonances we study in this paper we will refer to them as *elastic* CIRs.

A common experimental approach [12] to characterize such resonances has been to look for increased loss of atoms caused by enhanced three-body recombination in the vicinity of the resonance. However, this interpretation of the observed losses has been called into question by a recent experiment which observed a splitting of loss features under transversally anisotropic confinement [12], although later theoretical works showed that

no such splitting of elastic CIR can occur [13, 14]. One proposed explanation for the splitting is based on the fact that the trapping potentials used in experiments are not perfectly harmonic. This leads to a coupling of center-of-mass (COM) and relative (REL) motion [15–17], which in turn can lead to a coupling of two atoms in the ground state of the trap to a weakly bound molecular state with a COM excitation [18] (further elaborated on in [19]). The occupation of the bound state is only possible because the excess binding energy can be transferred into COM excitation energy due the anharmonicity of the confining potential. This redistribution of binding energy to kinetic energy is an inelastic process and thus we refer to these COM-REL coupling resonances as *inelastic* CIR.

In a many-body system losses at the inelastic CIR can be described as a two-step process: First, two atoms coherently couple to the COM-excited molecular state. Then, this molecule collides either with another molecule or an unbound atom, which leads to a deexcitation of the molecule into a deeply bound state and subsequent loss of the involved particles from the trap.

However, also different theoretical models have been developed to explain the observed splitting of the loss features in [12]. These argue with enhanced three-body effects in the vicinity of elastic CIR. One is based on multichannel effects [20], others [12, 21] on a Feshbach-type mechanism. In a many-body system as used in [12] different loss mechanisms are in principle possible and cannot be clearly distinguished by the experiment. A straightforward, yet experimentally challenging solution to this problem is to eliminate three-body effects by investigating a pure 2-body system. In this work we provide a direct experimental confirmation of the theory developed in [18] by performing a theoretical and experimental study of two  $^6\text{Li}$  atoms in an elongated trapping potential with a slight ellipticity. Ab initio calculations of the coupling

strengths, the widths and the positions of the coherent molecule formation at the inelastic CIR are found to be in quantitative agreement with the experimental results.

To prepare a quasi-1D two-body system we follow the same preparation scheme as described in [10, 22], which has a fidelity of about 90%. The two particles are trapped in the ground state of a cigar-shaped potential with a mean transversal confinement length of  $d_{\perp} = 0.486 \pm 0.006 \mu\text{m}$  and an aspect ratio of about 10:1, which is well in the quasi-1D regime [23]. The shape and anharmonicity of the potential have been characterized by precise measurements of the transition frequencies for exciting a single particle into the first and second excited level in the longitudinal and both transversal directions [24].

This two-body system is in absolute coordinates described by the Hamiltonian

$$H(\mathbf{r}_1, \mathbf{r}_2) = T_1(\mathbf{r}_1) + T_2(\mathbf{r}_2) + V_1(\mathbf{r}_1) + V_2(\mathbf{r}_2) + U(|\mathbf{r}_1 - \mathbf{r}_2|) \quad (1)$$

where  $T_1$ ,  $T_2$ ,  $V_1$ ,  $V_2$  denote the kinetic energies and potential energies due to the trap of particles one and two, respectively, and  $U$  the interatomic interaction. It has been demonstrated that sextic potentials, i.e. expansions of a  $\sin^2$  optical-lattice potential up to order six,

$$V(\mathbf{r}) = \sum_{j=x,y,z} \frac{2}{45} V_j k_j^6 j^6 - \frac{1}{3} V_j k_j^4 j^4 + V_j k_j^2 j^2, \quad (2)$$

are well suited to describe anharmonicity induced COM-REL coupling in single-well potentials [25], like the one used in our experiment.

The stationary Schrödinger equation for the Hamiltonian (1) can be solved exactly by the computational approach described in [26]. Herein, the interaction potential is treated by a numerically given Born-Oppenheimer potential curve of a  ${}^6\text{Li}$  system. The variation of the scattering length due to the magnetic Feshbach resonance can be modeled computationally by modifying the inner wall of the potential curve which effectively changes the scattering length of the system to arbitrary values [27].

For a two-particle system it is convenient to transform the Hamiltonian in REL and COM coordinates,  $\mathbf{r} = \mathbf{r}_1 - \mathbf{r}_2$  and  $\mathbf{R} = \frac{1}{2}(\mathbf{r}_1 + \mathbf{r}_2)$ , respectively,

$$H(\mathbf{r}, \mathbf{R}) = T_{\text{REL}}(\mathbf{r}) + T_{\text{COM}}(\mathbf{R}) + V_{\text{REL}}(\mathbf{r}) + V_{\text{COM}}(\mathbf{R}) + U_{\text{int}}(r) + W(\mathbf{r}, \mathbf{R}). \quad (3)$$

$V_{\text{REL}}(\mathbf{r})$  and  $V_{\text{COM}}(\mathbf{R})$  are the separable parts of the sextic potential [25]. Thus,  $W(\mathbf{r}, \mathbf{R})$  contains only the non-separable terms, i.e. a polynomial in  $r_j^2 R_j^2$ ,  $r_j^2 R_j^4$  and  $r_j^4 R_j^2$ . The potential parameters  $V_j$  and  $k_j$  are obtained by fitting the eigenenergies of a single particle in a sextic potential to the experimentally measured transition energies of a single particle in the trap. The fit results are given in [24]. The eigenenergies and wavefunctions of

the Hamiltonian (3) can now be calculated via exact diagonalization for different values of the s-wave scattering length. A fully coupled spectrum is shown in Fig. 1.

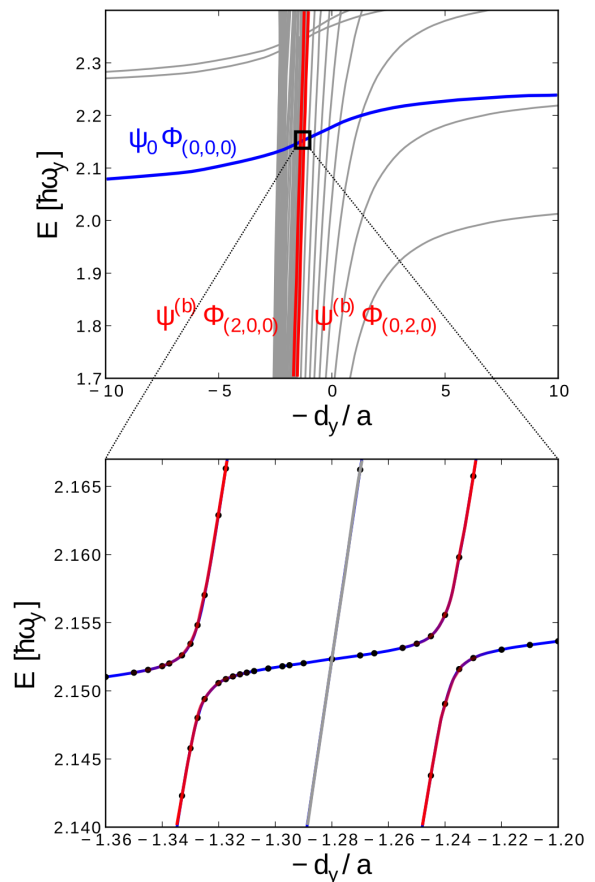


Figure 1. (color online) Eigenenergy spectrum of the Hamiltonian (3) for  ${}^6\text{Li}$  atoms confined in a sextic trapping potential. In the upper part all states bending down to  $-\infty$  are molecular states originating from the REL bound state  $\psi^{(b)}$  with different COM excitations. The two bound states marked in red are the only ones which have a significant coupling to the repulsive state (blue). For the other states (gray) the coupling is negligible. The magnified part shows the avoided crossings responsible for the COM-REL resonances.

Relative motion bound states  $\psi^{(b)}$  with COM excitation  $\Phi_{\mathbf{n}}$ ,  $\mathbf{n} = (n_x, n_y, n_z)$  (i.e. states bending down to negative infinity) cross with trap states, i.e. states whose energy converges asymptotically to a constant value for  $a \rightarrow 0^+$ . In the absence of a trapping potential these states would lie in the continuum. The system is initially in the lowest trap state, i.e. dominantly in the relative motion repulsive state  $\psi_0$  and COM ground state  $\Phi_{(0,0,0)}$  (see blue state in Fig. 1). Hence, it suffices to consider crossings with this state. The coupling, and equivalently the size of the avoided crossings, is described by the coupling matrix elements

$$W_{\mathbf{n}} = \langle \psi^{(b)} \Phi_{\mathbf{n}} | W | \psi_0 \Phi_{(0,0,0)} \rangle. \quad (4)$$

In [18] it was demonstrated that in quasi 1D only the lowest transversally COM excited bound states,  $|\psi^{(b)} \Phi_{(2,0,0)}\rangle$  and  $|\psi^{(b)} \Phi_{0,2,0}\rangle$  (see red states in Fig. 1), couple significantly with the lowest trap state. Therefore, in Fig. 1 only the transversally excited bound states form significant avoided crossings with the repulsive trap state. Due to the transverse anisotropy of the trap these crossings are non-degenerate which results in a splitting of the resonances. Such a splitting was also observed in [12] in quantitative agreement with the positions of the inelastic CIR [18].

To demonstrate that the crossing states possess characteristics of a bound and a trap state the mean radial density

$$\bar{r} = \int_0^\infty dr r \rho(r). \quad (5)$$

was calculated. Here,

$$\rho(r) = r^2 \int dV_{\mathbf{R}} d\Omega_{\mathbf{r}} |\Psi(\mathbf{r}, \mathbf{R})|^2 \quad (6)$$

is the radial pair density where  $\Psi(\mathbf{r}, \mathbf{R})$  denotes the full six-dimensional wavefunction of the system,  $dV_{\mathbf{R}}$  is the COM volume element and  $d\Omega_{\mathbf{r}}$  is the angular volume element of the REL motion. At  $d_y/a = 1.38$  the bound state has a mean radial distance of  $\bar{r} = 0.29 d_{\perp}$ , i.e. it is small compared to the mean transversal confinement length. This demonstrates the strong binding of the atoms. In the trap state, the atoms possess a mean distance of  $\bar{r} = 1.19 d_z = 3.06 d_{\perp}$ . This mean distance which is of the order of the longitudinal trap length  $d_z = 1.25 \mu\text{m}$  is a consequence of the elongated trap.

In the vicinity of the avoided crossing the system can be approximately described as a two-level system because the other states are energetically almost inaccessible. When the scattering length is ramped non-adiabatically towards the crossing and stopped in the gap region of the avoided crossing the system finds itself in a coherent superposition of the two adiabatic states [28], which in our case are the bound state  $|\psi^{(b)} \Phi_{\mathbf{n}}\rangle$  and the repulsive trap state  $|\psi_0 \Phi_{(0,0,0)}\rangle$ . Since both states evolve with different phase a Rabi-oscillation between the states occurs with the frequency

$$\Omega = \frac{1}{\hbar} \sqrt{W_{\mathbf{n}}^2 + \delta^2} \quad (7)$$

which is a measure for the coupling strength for  $\delta = (E_b - E_t)/2 = 0$ . Here,  $W_{\mathbf{n}}$  is the coupling matrix element from Eq. (4) while  $E_b$  and  $E_t$  denote the energies of the diabatic bound and trap states, respectively.

Experimentally this coherent superposition is realized by first preparing two  ${}^6\text{Li}$  atoms in the ground state of the potential and then increasing the scattering length  $a$  by ramping up the magnetic offset field non-adiabatically

with a speed of 20 G/ms. To locate the molecule formation resonances the ramp is suddenly stopped at different values of the magnetic offset field. The population is expected to oscillate between the unbound and the COM-excited molecular state as a function of the Rabi frequency  $\Omega$  which depends on the magnetic field.

In a first experiment we wait for a fixed hold time of 12.5 ms after stopping the ramp at different magnetic field values between 779 G and 788 G [29]. We then measure the number of free atoms remaining in the ground state of the trap by ramping to a magnetic field of 523 G where the molecules are deeply bound and therefore not observed with our detection scheme. Thus, the mean number of molecules is given by  $N_{\text{mol}} = (N_0 - N_{\text{GS}})/N_0$ , where  $N_0$  is the mean number of atoms in the initial system and  $N_{\text{GS}}$  is the mean number of particles detected in the non-molecular ground state at the end of the experiment. To check whether the missing atoms indeed end up in the molecular state we repeated the experiment but ramped the magnetic field to a value of 900 G before measuring the number of particles. At this magnetic field we are far above the elastic CIR so that the molecules become weakly bound and the constituent particles of the molecules can be detected with our detection scheme. We found that there is no measurable change compared to the initial particle number when measuring above the elastic CIR, which excludes the presence of any significant loss channels in our system. Figure 2 shows the detected number of particles in the repulsive state depending on the magnetic offset field. As expected from numerics, two peaks are observable which are identified as the COM-REL motion coupling resonances created by the two molecular states excited in  $x$ - and  $y$ - direction of the anisotropic confinement.

To analyze the dynamics of the coupling we ramped to different values of the magnetic offset field around the features shown in Fig. 2 and held the system for different hold times. With less than 10% probability we detect only a single atom in the trap, i.e. the two atoms are either free ( $N = 2$  detected) or bound to a molecule ( $N = 0$ ). The few realizations with just a single atom detected ( $N = 1$ ) are not considered in the analysis. Fig. 3 a) shows the result of one of these measurements. The oscillation of the fraction of molecules shows that we have created a coherent superposition of the molecular and the repulsive state. By performing a sinusoidal fit to the data we can extract the Rabi frequency  $\Omega$  of the oscillation. The maximum amplitudes of the oscillation for different magnetic fields are shown in figure 3 b). From a Lorentzian fit to the amplitude we can extract the width (FWHM) of the coupling in terms of the magnetic offset field. Table I shows the width of the coupling resonances determined from the measurement. The spacing between the two resonances, see Table I, is in agreement up to 0.3 G with the numerical calculation. The absolute position of the experimental resonances is shifted about

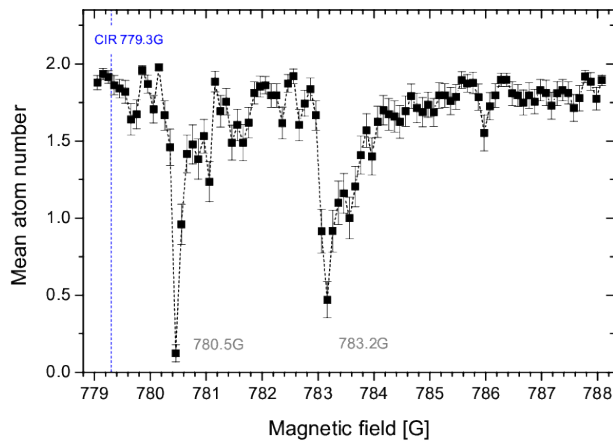


Figure 2. Disappearance of particles in the repulsive non-bound state. Due to the COM-REL motion coupling the particles in the non-bound state couple into a molecule and disappear when detecting the number of particles in the non-bound state. One observes two peaks indicating COM-REL motion coupling resonances involving two excited molecular states in  $x$ - and  $y$ -direction of the confinement. Each data point is the average of about 50 individual measurements with discrete atom number. The blue dashed line indicates the position of the elastic CIR at  $779.3 \pm 0.5$  G calculated using the transversal confinement length  $d_{\perp}$  and the calibration of the scattering length  $a(B)$  of [30] as inputs for the theory of [31].

COM excitation	Position [G]		FWHM[G]		$\Omega_0/2\pi$ [Hz]	
	exp.	num.	exp.	num.	exp.	num.
(0, 2, 0)	780.5	776.01	0.25(0.03)	0.35	83(2)	64
(2, 0, 0)	783.2	779.02	0.42(0.06) <sup>(*)</sup>	0.35	75(1) <sup>(*)</sup>	69

Table I. Comparison between experiment and numerical calculation. <sup>(\*)</sup> See [24] for these measurements.

4.3 G compared to the theoretical values. In view of the width of the elastic CIR[32] of 250 G this is a remarkable accuracy. Moreover, except for the two COM-REL coupling resonances no significant molecule formation was observed over the whole width of the elastic CIR.

In conclusion, our results directly show that in a two-particle system the COM-REL coupling allows for the coherent coupling of an unbound atomic pair and a molecular state without a third particle being present. Competing processes such as three-body recombination or processes involving atoms in higher bands [20] are excluded by our high preparation fidelity. Hence, the agreement between the theoretical and experimental results gives a quantitative confirmation of the theory of inelastic CIR [18]. Furthermore, our results show that a molecule formation in a two-body system is absent at the elastic CIR [33]. The results strongly imply that the inelastic resonances are the dominant cause for the appearance of the two distinct loss features in the experiment by E. Haller et al. [12] as was already suggested in [18]. In gen-

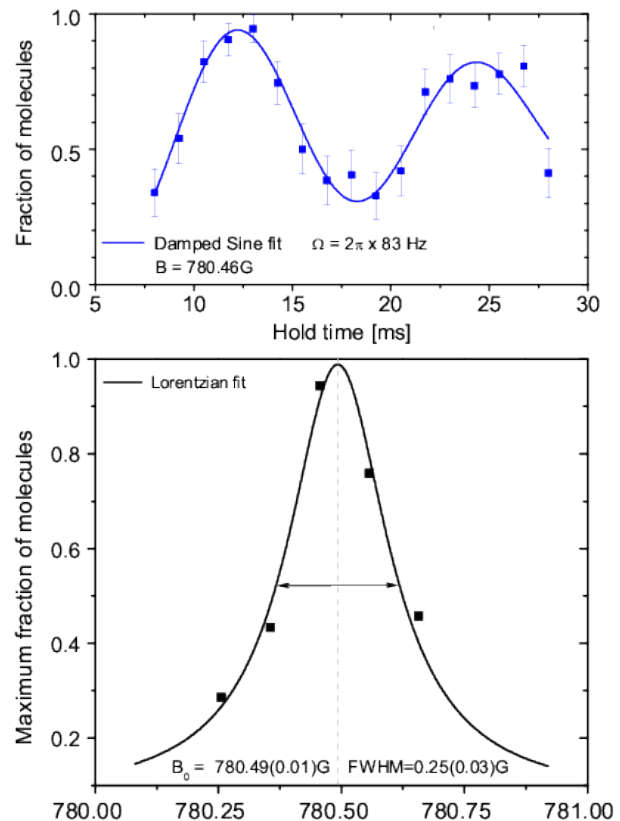


Figure 3. Coherent dynamic of the COM-REL motion coupling. (a) Oscillation between the non-bound and the COM excited molecular state. From a sinusoidal fit we deduce the Rabi-frequency  $\Omega$ . (b) Maximum amplitude of the oscillation. The data points are extracted from measurements analog to figure a) at different magnetic offset fields.

eral, the effect of COM-REL motion coupling can have a significant impact on the stability of 1D quantum gases and should therefore be considered in current 1D experiments.

The authors gratefully acknowledge support from the *Else-Neumann Stiftung, Studienstiftung des deutschen Volkes, Fonds der Chemischen Industrie*, IMPRS-QD, Helmholtz Alliance HA216/EMMI, the Heidelberg Center for Quantum Dynamics and ERC Starting Grant 279697. We thank M. Gärttner for helpful discussions.

\* ssala@physik.hu-berlin.de

- [1] M. Olshanii, Phys. Rev. Lett. **81**, 938 (1998).
- [2] B. Paredes, A. Widera, V. Murg, O. Mandel, S. Fölling, I. Cirac, G. V. Shlyapnikov, T. W. Hänsch, and I. Bloch, Nature **429**, 277 (2004).
- [3] T. Kinoshita, T. Wenger, and D. S. Weiss, Science **305**, 1125 (2004).
- [4] T. Kinoshita, T. Wenger, and D. S. Weiss, Phys. Rev. Lett. **95**, 190406 (2005).

- [5] E. Haller, M. Gustavsson, M. J. Mark, J. G. Danzl, R. Hart, G. Pupillo, and H. Nägerl, *Science* **325**, 1224 (2009).
- [6] T. Kinoshita, T. Wenger, and D. S. Weiss, *Nature* **440**, 900 (2006).
- [7] T. Stöferle, H. Moritz, K. Günter, M. Köhl, and T. Esslinger, *Phys. Rev. Lett.* **96**, 030401 (2006).
- [8] C. Ospelkaus, S. Ospelkaus, L. Humbert, P. Ernst, K. Sengstock, and K. Bongs, *Phys. Rev. Lett.* **97**, 120402 (2006).
- [9] E. Haller, R. Hart, M. J. Mark, J. G. Danzl, L. Reichsöllner, M. Gustavsson, M. Dalmonte, G. Pupillo, and H.-C. Nägerl, *Nature* **466**, 597 (2010).
- [10] G. Zürn, F. Serwane, T. Lompe, A. N. Wenz, M. G. Ries, J. E. Bohn, and S. Jochim, *Phys. Rev. Lett.* **108**, 075303 (2012).
- [11] C. Chin, R. Grimm, P. Julienne, and E. Tiesinga, *Rev. Mod. Phys.* **82**, 1225 (2010).
- [12] E. Haller, M. J. Mark, R. Hart, J. G. Danzl, L. Reichsöllner, V. Melezhik, P. Schmelcher, and H.-C. Nägerl, *Phys. Rev. Lett.* **104**, 153203 (2010).
- [13] S.-G. Peng, S. S. Bohloul, X.-J. Liu, H. Hu, and P. D. Drummond, *Phys. Rev. A* **82**, 063633 (2010).
- [14] W. Zhang and P. Zhang, *Phys. Rev. A* **83**, 053615 (2011).
- [15] V. Peano, M. Thorwart, C. Mora, and R. Egger, *New J. Phys.* **7**, 192 (2005).
- [16] P.-I. Schneider, S. Grishkevich, and A. Saenz, *Phys. Rev. A* **80**, 013404 (2009).
- [17] J. P. Kestner and L.-M. Duan, *New J. Phys.* **12**, 053016 (2010).
- [18] S. Sala, P.-I. Schneider, and A. Saenz, *Phys. Rev. Lett.* **109**, 073201 (2012).
- [19] S.-G. Peng, H. Hu, X.-J. Liu, and P. D. Drummond, *Phys. Rev. A* **84**, 043619 (2011).
- [20] V. S. Melezhik and P. Schmelcher, *Phys. Rev. A* **84**, 042712 (2011).
- [21] V. Dunjko, M. G. Moore, T. Bergeman, and M. Olshanii, in *Advances in Atomic, Molecular, and Optical Physics*, *Advances In Atomic, Molecular, and Optical Physics*, Vol. 60, edited by P. B. E. Arimondo and C. Lin (Academic Press, 2011) pp. 461 – 510.
- [22] F. Serwane, G. Zürn, T. Lompe, T. B. Ottenstein, A. N. Wenz, and S. Jochim, *Science* **332**, 336 (2011).
- [23] Z. Idziaszek and T. Calarco, *Phys. Rev. A* **74**, 022712 (2006).
- [24] See Supplemental Material for details.
- [25] S. Grishkevich and A. Saenz, *Phys. Rev. A* **80**, 013403 (2009).
- [26] S. Grishkevich, S. Sala, and A. Saenz, *Phys. Rev. A* **84**, 062710 (2011).
- [27] S. Grishkevich, P.-I. Schneider, Y. V. Vanne, and A. Saenz, *Phys. Rev. A* **81**, 022719 (2010).
- [28] N. Syassen, D. M. Bauer, M. Lettner, D. Dietze, T. Volz, S. Dürr, and G. Rempe, *Phys. Rev. Lett.* **99**, 033201 (2007).
- [29] The duration of the hold time is such that it corresponds to a half-cycle (i.e. a  $\pi$ -pulse) of an expected Rabi-Frequency of  $\Omega_0 = 2\pi \times 80$  Hz.
- [30] G. Zürn, T. Lompe, A. N. Wenz, S. Jochim, P. S. Julienne, and J. M. Hutson, *ArXiv:1211.1512*.
- [31] T. Bergeman, M. G. Moore, and M. Olshanii, *Phys. Rev. Lett.* **91**, 163201 (2003).
- [32] The width of the elastic CIR is mainly determined by the width of the Feshbach resonance [11].
- [33] One should note that this is no contradiction to the description of the elastic CIR using a Feshbach type mechanism [31]. In this picture a shifted bound state crosses the continuum threshold which one could expect to be responsible for molecule formation. However, this shifted bound state of [31] is *not* an eigenstate of the full Hamiltonian but of a modified one which results from a non-unitary transformation and hence does not couple to the repulsive trap state. In contrast, the molecular states that are populated in the present work are bound states with COM excitation, i.e. eigenstates of the full Hamiltonian, that couple to the repulsive state due to the anharmonic trapping potential which manifests in avoided crossings, see Fig. 1.
- [34] G. Zürn, PhD thesis, Ruprecht-Karls Universität Heidelberg.

## SUPPLEMENTAL MATERIAL

### Measurement of the single particle excitation frequencies in the trap

We excite individual atoms in the ground state of the trap to higher trap states by periodically modulating the center position or the confinement length of the trap with a certain frequency  $\omega$ . The transition frequencies are determined from fits to the excitation spectra (see [34]). The results are given in Table II

h.o. number ( $n_x, n_y, n_z$ )	frequency $\omega/2\pi$ [kHz]
(0,0,1)	1.486(0.011)
(0,0,2)	2.985(0.010)
(0,0,4)	2.897(0.020)
(1,0,0)	13.96(0.08)
(0,1,0)	14.82(0.09)
(2,0,0)	26.43(0.27)
(0,2,0)	28.26(0.25)

Table II. Transition frequencies in the trap of atoms excited in the trap. We denote the transitions by the corresponding quantum number of a harmonic oscillator.

### Determination of the elastic CIR

To determine the elastic CIR we only consider one resonance following [13, 14] although we have found an anisotropy in our system. We calculate the position of the elastic CIR from the transversal confinement length

$$d_{\perp} = \sqrt{\hbar/\mu\omega_{\perp}}. \quad (8)$$

To determine the mean trap frequency  $\omega_{\perp}$  we fit the Gaussian shape of the optical beam which creates the trapping potential to the measured transition frequencies (see [34]). From the two profiles in radial direction we deduce the corresponding transition frequencies between the lowest single particle bound states in the gaussian potential and calculate the mean frequency

$$\omega_{\perp} = \frac{1}{2}(\omega_{(1,0,0)\text{fit}} + \omega_{(0,1,0)\text{fit}}) = 2\pi \times (14.22 \pm 0.35) \text{ kHz}. \quad (9)$$

Using equation 8 as the input of the theory of [31] and the calibration a(B) of [30] we calculate the position of the elastic CIR. The propagated error of the mean trap frequency serves as the systematic uncertainty of the position of the CIR.

### Fitting the trapping potential

In an ideal and simplified case, the shape of the external potential is determined by the profile of a Gaussian beam which results in the potential

$$V(\mathbf{r}) = V_0 \left( \frac{w_0}{w(z)} \right)^2 \exp \left( \frac{-2(x^2 + y^2)}{w^2(z)} \right) \quad (10)$$

where  $w(z) = w_0 \sqrt{1 + \left( \frac{z}{z_R} \right)^2}$  and  $w_0 = w(0)$  is the waist size of the beam and  $z_R = \frac{\pi w_0^2}{\lambda}$  is the Rayleigh range. The measurement of the excitation energies, Table II, reveals an ellipticity of  $\omega_{x2-0}/\omega_{y2-0} = 1.07$  in radial direction which cannot be justified by the beam potential Eq. (10). Hence, for the theoretical description, the potential Eq. (10) is expanded in a Taylor series around the origin up to second order which results in a harmonic potential of the form

$$V(\mathbf{r}) = \frac{\hbar}{2} \sum_{j=x,y,z} \omega_j^2 j^2. \quad (11)$$

To address the ellipticity in the radial direction, different harmonic  $\omega_j$  frequencies for the  $x$  and  $y$  direction are chosen. In the harmonic approximation, however, the coupling between COM and REL degrees of freedom vanishes. This is surely not the case for the finite, anharmonic experimental potential. Hence, for the model potential higher order terms are introduced to include COM-REL coupling. It has been demonstrated that sextic potentials, i.e. expansions of a  $\sin^2$  optical lattice potential up to order six

$$V(\mathbf{r}) = \sum_{j=x,y,z} \frac{2}{45} V_j k_j^6 j^6 - \frac{1}{3} V_j k_j^4 j^4 + V_j k_j^2 j^2, \quad (12)$$

are well suited to describe single well potentials including COM-REL coupling [25].

The resulting fitting parameters (given in atomic units) are  $k_x = 9.23 \times 10^{-5}$  a.u.,  $k_y = 8.77 \times 10^{-5}$  a.u.,  $k_z = 1.58 \times 10^{-5}$  a.u.,  $V_x = 6.82 \times 10^{-12}$  a.u.,  $V_y = 6.58 \times 10^{-12}$  a.u. and  $V_z = 2.33 \times 10^{-12}$  a.u.

### COM-REL coupling involving the state $|\psi^{(b)} \Phi_{2,0,0}\rangle$

The measurement of coherent coupling between the repulsive non-bound state and the COM-excited bound state  $|\psi^{(b)} \Phi_{2,0,0}\rangle$  has been performed in a similar way as the one presented in the main text with the only difference that an additional linear potential had been applied in  $z$ -direction (see Fig.4). The additional potential reads

$$V_{\text{lin}} = \mu_m B' z \quad (13)$$

where  $\mu_m$  is the Bohr magneton and  $B' = 18.92$  G/cm a magnetic field gradient. The additional potential

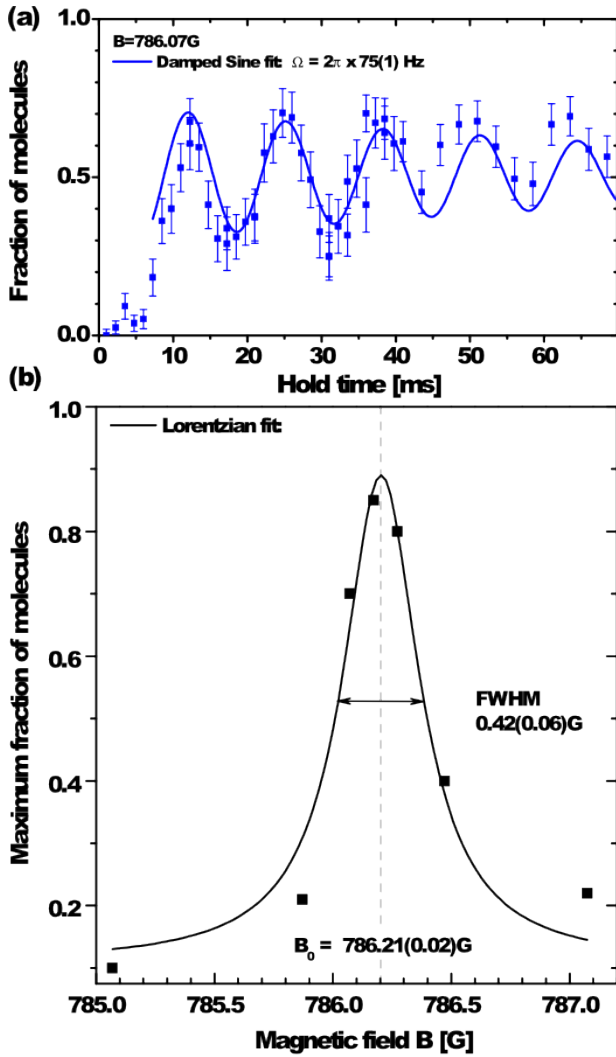


Figure 4. Dynamic of the COM-REL motion coupling. (a) Oscillation between the non-bound state and the COM excited molecular state  $|\psi^{(b)} \Phi_{2,0,0}\rangle$ . (b) Maximum fraction of molecules extracted from measurements similar to a) at different magnetic fields.

slightly shifts the energy of the non-bound repulsive state  $|\psi_{(0)} \Phi_{0,0,0}\rangle$  and thus also shifts the position of the COM-REL coupling resonances. Yet, the influence on the coupling strength should be negligible. Hence we can use the results for the Rabi frequency and the width presented in Fig. 4 for a comparison with the numerical calculation which has been performed without an additional potential in z-direction.